The depolarization - attenuated backscatter relation: CALIPSO lidar measurements vs. theory

Yongxiang Hu, Mark Vaughan, Zhaoyan Liu, Bing Lin, Ping Yang, David Flittner, Bill Hunt, Ralph Kuehn, Jianping Huang, Dong Wu, Sharon Rodier, Kathy Powell, Charles Trepte, and David Winker

NASA Langley Research Center, Hampton, VA 23681
Yongxiang.hu-1@nasa.gov

Abstract: Using measurements obtained by the Cloud-Aerosol Lidar and Infrared Pathfinder Satellite Observations (CALIPSO) satellite, relationships between layer-integrated depolarization ratio (δ) and layer-integrated attenuated backscatter (γ') are established for moderately thick clouds of both ice and water. A new and simple form of the δ–γ' relation for spherical particles, developed from Monte Carlo simulations and suitable for both water clouds and spherical aerosol particles, is found to agree well with the observations. A high-backscatter, low-depolarization δ–γ' relationship observed for some ice clouds is shown to result primarily from horizontally oriented plates and implies a preferential lidar ratio – depolarization ratio relation in nature for ice cloud particles containing plates. ©2007 Optical Society of America

OCIS codes: (010.3640) Lidar; (290.1090) Aerosol and cloud effects; (290.4210) Multiple scattering.

References and links

1. R. Schotland, et al., "Observations by lidar of linear depolarization ratios for hydrometers," J. Appl. Meteorol. **10**, 1011–1017 (1971).
2. Y. Hu, et al., "Identification of cloud phase from PICASSO-CENA lidar depolarization: A multiple scattering sensitivity study," J. Quant. Spectrosc. Radiat. Transfer **70**, 569-579 (2001).
3. Y. Hu, et al., "Using Backscattered Circular Component for Cloud Particle Shape Determination: A Theoretical Study," J. Quant. Spectrosc. Radiat. Transfer **79-80**, 757-764 (2003).
4. D. M. Winker et al., "The CALIPSO mission: Spaceborne lidar for observation of aerosols and clouds," Proc. SPIE **4893**, 1-11 (2003).
5. Y. Hu et al., "A simple relation between lidar multiple scattering and depolarization for water clouds," Optics Letters **31**, 1809-1811 (2006).
6. C. M. R. Platt, et al., "Backscatter to extinction ratios in the top layers of tropical mesoscale convective systems and in isolated cirrus from LITE observations," J. App. Meteorol. **38**, 1330-1345. (1999).
7. R. G. Pinnick, et al., "Backscatter and extinction in water clouds," J. of Geoph. R. **88**, 6787-6796 (1983).
8. Y. Hu et al., "A simple multiple scattering-depolarization relation of water clouds and its potential applications," Proceedings of 23nd International Laser Radar Conference, Nara, Japan, 19-22 (2006).
9. E. J. O'Connor, et al., "A technique for autocalibration of cloud lidar," J. Atmos. Oc. T. **21**, 777-786 (2004).
10. C. M. R. Platt, "Lidar Observation of a Mixed-Phase Altostratus cloud," J. Appl. Meteorol. **16**, 339-345 (1977).

1. Introduction

Lidar measurements of depolarization ratio provide highly reliable information about cloud ice-water phase [1]. The basic assumption is that nonspherical particles depolarize the backscattered light, whereas spherical particles do not. However, this assumption is valid

only when the signal is dominated by single scattering. When significant multiple scattering is present, even spherical particles generate depolarized signals, thus confounding the task of cloud phase discrimination. Due to the large footprints typical of space-based viewing geometries, multiple scattering effects on space-borne lidar measurements [2,3], such as those made by the Cloud-Aerosol Lidar and Infrared Pathfinder Satellite Observations (CALIPSO) [4] satellite, can be significant.

Because theoretical computations of multiple scattering contributions to the lidar signal are quite time-consuming, most operational lidar retrieval algorithms incorporate an empirical parameterization of multiple scattering effects. Our previous study characterized multiple scattering for spherical particles using a polynomial relation between layer-integrated depolarization, $\delta = \int_{top}^{base} \beta'_\perp(r)\,dr \Big/ \int_{top}^{base} \beta'_\parallel(r)\,dr$, and layer-integrated attenuated backscatter[5], $\gamma' = \int_{top}^{base} \beta'_\perp(r) + \beta'_\parallel(r)\,dr$. This work was based on Monte Carlo simulations and ground-based multiple-field-of-view (MFOV) lidar measurements. Recently we have discovered a more concise and physically meaningful expression for the δ–γ relation for spherical particles. In this paper we compare this new theoretical relationship with CALIPSOs lidar measurements of water clouds. We also present a new and significantly different relationship observed between depolarization and backscattering from ice clouds and provide an interpretation of the major features of the relation.

2. The multiple scattering – depolarization relation for spherical particles

Our previous study[5] introduced a polynomial relationship between a layer-integrated back-scatter factor, A_s, and the layer-integrated depolarization ratio, δ, for water clouds and spherical aerosols, as follows:

$$A_s = \frac{\gamma_{ss}}{\gamma'} = 0.999 - 3.906\,\delta + 6.263\,\delta^2 - 3.554\,\delta^3. \tag{1}$$

The layer-integrated total attenuated backscatter, γ', is measured by the lidar, and is equal to the sum of the single scattering contribution, γ_{ss}, and the multiple scattering contributions, γ_{ms}. This same relation can be further simplified as

$$\frac{1}{A_S} = \frac{\gamma_{ss} + \gamma_{ms}}{\gamma_{ss}} = \frac{\gamma'}{\gamma_{ss}} = \left(\frac{1+\delta}{1-\delta}\right)^2. \tag{2}$$
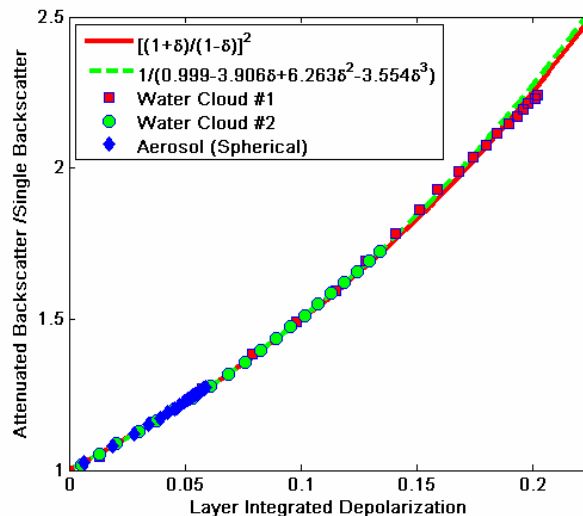
Fig. 1. Relationship between layer-integrated depolarization and attenuated backscatter for spherical cloud particles derived from Monte Carlo simulations. The green dashed line is from previous work (Hu et al. 2006). The solid red line is the revised form of the same relation reported in this work.

This simplified form of the relation applies to atmospheric lidar returns from spherical particles (cloud droplets and liquid aerosol particles), irrespective of extinction coefficient and effective particle size (Fig. 1). The new formulation (red solid line in Fig. 1) also agrees well with the previously published polynomial relation (green dashed line). Monte Carlo simulations confirm the suitability of the relation for spherical particles measured using various satellite and aircraft viewing geometries [5]. This is demonstrated in Fig. 1, which shows two satellite-viewing cases of water clouds with different extinction coefficients (red squares for high extinction coefficient and green circle for lower extinction coefficient) and a very weakly absorbing aerosol (blue diamond) with refractive index = 1.4+0.001i.

Equation (2) is valid not only for integrated returns of the entire layer, but also for the integrated returns from the top of the layer to any level inside the cloud/aerosol layer for measurements made with a lidar system of relatively short transient response.

3. Comparisons with CALIPSO lidar measurements

The above relation between multiple scattering and depolarization can be verified by analyzing CALIPSO lidar measurements of opaque water clouds. These clouds are relatively tractable, because the single scattering contribution, γ_{ss}, required in expressions (1) and (2) can be reasonably estimated from the relation $\gamma_{ss}=(1-T^2)/(2S_c)$ [5, 6]. Here T^2 is the two-way transmittance between the satellite and the cloud base (assumed to be 0 for totally attenuating layers) and S_c is the extinction-to-backscatter ratio of water clouds. For measurements made at 532 nm, S_c has a value very close to 19 sr^{-1} for most water clouds [7, 8, 9]. At 1064 nm, S_c lies between 18 sr^{-1} and 19 sr^{-1}.
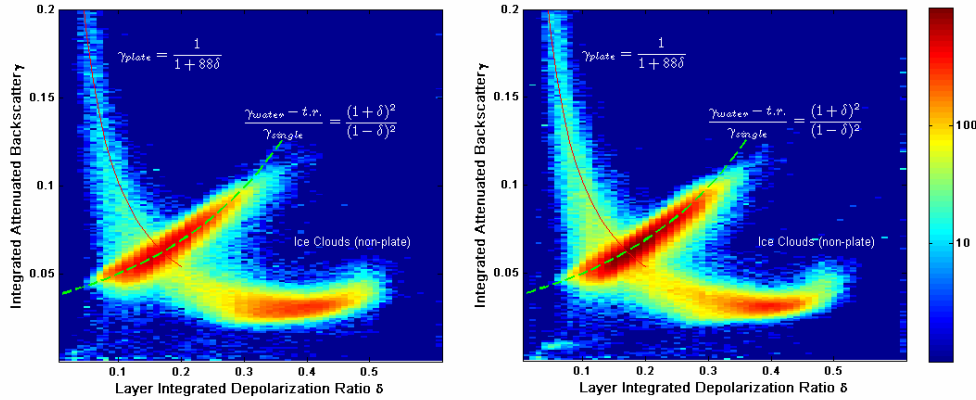
Fig. 2. Summary statistics showing the δ–γ′ relationship for opaque clouds detected during the months of July (left panel) and October (right panel) 2006. The color of each pixel represents the frequency of occurrence for a Δδ–Δγ′ box measuring 0.001-by-0.01 sr^{-1}. The green dashed line indicates the δ–γ′ relation for water clouds, as described by theory. Red dotted line: ice cloud δ-β relation with least square fit.

Fig. 2 shows the statistics of the relation between layer-integrated attenuated backscatter at 532 nm and layer-integrated depolarization ratio for opaque clouds (both water and ice) for all CALIPSO observations from July (left panel) and October (right panel) of 2006. Opaque clouds are identified by the lack of a surface return signal beneath the cloud layer. The color of each pixel represents the frequency of occurrence. The relation between the layer-integrated depolarization and the layer-integrated attenuated backscatter in Fig. 2 is well clustered into two distinct groups:

1. Water clouds around the green dashed line with positive slope.
2. Ice clouds around the red solid line with mostly negative slope .

The red solid lines in both panels of Fig. 2 show least square fits to the downward-sloping branch of the δ–γ′ relationship for all opaque ice clouds (optical depth greater than ~4) detected by the CALIPSO lidar, approximated using the empirically derived function

$$\gamma' = \frac{1}{1 + 88\,\delta}\,.$$

(3)

The horizontal branch of the δ–γ′ relationship for ice clouds, in the lower central and right areas of the plot, is due to clouds composed of randomly oriented ice crystals. In these clouds the depolarization is dependent primarily on ice crystal habit and is either independent of or slightly positively correlated with the integrated signal strength. The data points in this high backscatter, low depolarization region in the upper left hand of the plots represent ice clouds for which the signal characteristics are primarily due to the presence of horizontally oriented plate crystals. In its standard flight configuration, the CALIPSO lidar is pointed to within 0.3° of nadir, and it is well known that specular reflections from oriented plates will not depolarize the lidar backscatter. [10] Furthermore, the extinction-to-backscatter ratio for horizontally oriented plates can be as small as 1 sr, and thus the integrated attenuated backscatter can become quite large. When multiple scattering effects are included, the effective extinction-to-backscatter ratio can approach 0.5 sr. This occurs because a significant fraction of the photons which are scattered by the crystals are scattered at very small angles and remain within the field of view of the lidar receiver. For opaque layers of horizontally aligned plates, the layer-integrated backscatter can be as high as 1 sr^{-1}. As the fraction of horizontally oriented plates within a cloud layer decreases, the layer-integrated depolarization increases, because the depolarization ratios for other ice particle shapes are significantly larger.

Similarly, the extinction-to-backscatter ratios of these other particles are also significantly larger (e.g., $S_c > 25$ sr, so that $1/(2S_c) < 0.02$ sr^{-1}). The layer-integrated attenuated backscatter thus decreases as the fraction of aligned plates decreases. Together, these behaviors explain the negative sloping relation between δ and γ' seen in the ice cloud data.

Consider now a cloud containing randomly oriented ice crystals and some arbitrary number of horizontally oriented plates. If the mean depolarization ratio of the randomly oriented particles is known, then the backscattering contributions of the horizontally oriented plates can be separated from the contributions made by the randomly oriented particles. To do this, we express the fractional contribution of the horizontally oriented plates to the total layer integrated attenuated backscatter as $1 - f$. Because the oriented plates do not depolarize the signal, the measured depolarization ratio, δ, is due entirely to the randomly particles within the layer, so that $\delta = f \cdot \delta_{ROP}$, where δ_{ROP} is the depolarization of the randomly oriented particles. The contribution of the horizontally oriented plates to γ' is therefore $1 - \delta/\delta_{ROP}$.

Equation (3) also implies that, when horizontally oriented plates are present, there is in nature a preferential lidar ratio–depolarization ratio relation for the remaining ice particles within the cloud. For an opaque ice cloud composed of both oriented plates and randomly oriented particles, γ' can be expressed as

$$\gamma' = \left(2(1-f)\eta_{plate}S_{plate} + 2f\eta_{MIP}S_{MIP}\right)^{-1} + o(\eta_{plate} - \eta_{MIP}).$$ (4)

Here η_{plate} and η_{ROP} are, respectively, the multiple scattering factors for oriented plates and for the remaining, randomly oriented ice particles. The difference in magnitude between the two multiple scattering factors is assumed to be small. Given that $2\eta_{plate}S_{plate} \to 1$, and considering $f = \delta/\delta_{ROP}$ and $\delta \ll 2\delta_{ROP}$, Eq. (3) leads to $2f\eta_{MIP}S_{MIP} - f = 88\delta$. The 'effective' lidar ratio, ηS, and integrated depolarization ratio for the randomly oriented ice particles are thus related by:

$$\eta_{MIP}S_{MIP} \approx 44\delta_{MIP}.$$ (5)

The green dashed lines in both panels of Fig. 2 and Fig. 3 are derived using

$$\frac{\gamma' - \gamma'_{TR}}{\gamma_{ss}} = \left(\frac{1+\delta}{1-\delta}\right)^2.$$ (6)

where γ'_{TR} is a correction term that compensates for a transient response artifact that occurs in the lidar receiver when very strong backscatter signals are detected. The effect shows up as a low-level, exponentially decaying "tail" on strong 532 nm backscatter profiles. This artifact is not seen in the 1064 nm channel. These transient response tails are estimated to contribute 0.0098 sr^{-1} to the layer-integrated 532 nm attenuated backscatter returns from dense water clouds and this contribution has been corrected for in the analytic curves overlaid on the water-cloud data.

The influence of horizontally oriented plates on the δ–γ' relationship for ice clouds is further revealed in Fig. 3. For this set of measurements, acquired during November 2006, the CALIPSO spacecraft was tilted so that the lidar was pointing at 3° off-nadir. Even at this relatively small off-nadir angle, specular reflections from horizontally oriented crystal facets are almost entirely eliminated, and as a result the ice cloud data that appears in the upper left quadrants of both panels in Fig. 2 (i.e., the low δ, very high γ' regions) all but vanishes in Fig. 3.
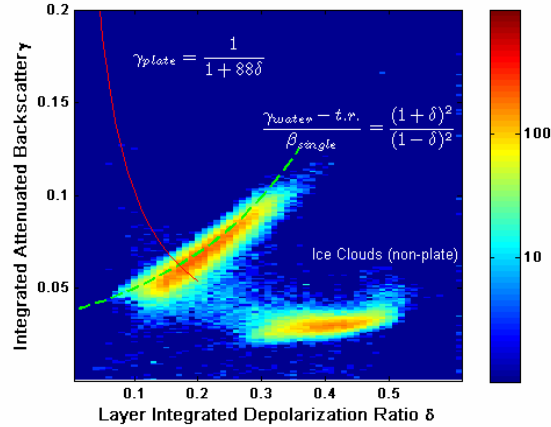
Fig. 3. Summary statistics showing the δ–γ' relationship for opaque clouds detected during the November 2006, when the pointing angle of the CALIPSO lidar was 3° off-nadir. The interpretation of the pixel colors in this image is the same as for Fig. 2.

4. Summary

In this article we have explored the relationships between depolarization and backscattering for both ice and water clouds using two months (one summer month and one fall month) of global lidar observations acquired by the CALIPSO satellite. The negative sloping branch of the δ–γ' relation for ice clouds is explained by the presence of horizontally oriented ice plates. It also implies a possible preferential ice cloud lidar ratio – depolarization ratio relationship in nature for ice clouds containing horizontally oriented plates. We have also introduced a simple form of the δ–γ' relation for spherical particles, including both clouds and aerosols, derived from Monte Carlo simulation. The positive correlations between depolarization and integrated attenuated backscatter for water clouds are consistent for the two months studied, and the measured relations agree well with the theoretical predictions. The difference in the statistics of the relation between July and October 2005 (Fig. 2) is very small in terms of relative location of the frequency of occurrence. This implies that the CALIPSO calibration has been very stable (possibly to within 2%).